

Enhanced Robust Model Predictive Control for Permanent Magnet Synchronous Motor Drives

Ruifang Chen¹ , Xiaoguang Zhang¹ 

¹North China University of Technology, China

²North China University of Technology, China

Corresponding author: Xiaoguang Zhang, zxg@ncut.edu.cn

Speaker: Ruifang Chen, 2022322070107@mail.ncut.edu.cn

Abstract

Traditional Model Predictive Control (MPC) methods are typically designed for high switching frequency environments to achieve precise control. However, high switching frequencies significantly increase inverter switching losses, leading to substantial heat generation and power loss, which reduces overall control performance. At low switching frequencies, traditional MPC methods struggle to maintain system robustness and high performance. To address these issues, this paper presents an improved model predictive voltage control (MPVC) method designed to maintain excellent dynamic and steady-state performance and robustness in permanent magnet synchronous motors (PMSMs) operating at low switching frequencies. The proposed method first accurately models the PMSM mathematically, then uses current differences to obtain real-time equivalent inductance and flux-linkage data. Next, an improved cost function is constructed to determine the optimal voltage vector to be applied to the motor while reducing the system's switching frequency. Simulation results validate the effectiveness and feasibility of this method.

1 Introduction

Permanent magnet synchronous motors (PMSMs) are widely used in industrial applications due to their high efficiency and power density [1]. Model predictive control (MPC) has become a research hotspot for PMSM control due to its excellent dynamic performance and ease of incorporating various constraints [2]. Traditional MPC methods are typically designed for high switching frequency environments to achieve precise dynamic control. However, high switching frequencies significantly increase inverter switching losses, leading to substantial heat and power losses, which not only reduce overall control performance but also pose significant challenges to heat dissipation design and system safety and reliability [3]. Finite-control-set MPC, which does not require pulse-width modulation, responds quickly and outputs only one state per control cycle, making it ideal for low switching frequency applications [4]. Nonetheless, maintaining system robustness and high performance at low switching frequencies, especially when dealing with system nonlinearity and parameter variations, remains challenging for traditional control methods [5].

To address these issues, various control methods have been proposed by researchers. For instance, low-frequency inverters have been extensively studied,

but control performance significantly decreases at lower frequencies due to increased discretization errors, which greatly reduce prediction accuracy [6]. In [7], a delay compensation method based on high-frequency square wave voltage injection is proposed, using a Luenberger observer to estimate speed and position. This method compensates for delay-induced errors by feedback of current-estimated delay angle errors, improving the performance of sensorless control systems at low switching frequencies. In [8], the application of model predictive torque control (MPTC) in PMSMs is explored. MPTC directly predicts torque and flux-linkage and incorporates them into the objective function to optimize torque control by selecting voltage vectors, while also introducing zero voltage vectors and duty cycle concepts to reduce torque ripple. However, this method increased parameter dependency and switching frequency, leading to higher heat and losses. In [9], an equivalent flux-linkage vector is constructed from torque and flux-linkage references. The required voltage vector reference is then obtained based on deadbeat flux control principles, and an optimal cost function was used to select the best voltage vector closest to the reference.

To enhance PMSM robustness at low switching frequencies, this paper proposes an improved MPC strategy. MPC, as an advanced control method, predicts future system behavior and optimizes control

inputs, effectively addressing system nonlinearity and disturbances, thus improving control accuracy and system robustness. This paper first establishes an accurate mathematical model of PMSM and uses current difference measurements to detect equivalent inductance and flux linkage data. An improved cost function is then constructed to select the optimal voltage vector while reducing the system's switching frequency, thereby enhancing the robustness of the motor system under low switching frequency conditions.

The structure of this paper is as follows: the second section introduces the basic and improved mathematical models of PMSM. The third section details the improved control strategy and its specific implementation steps. The fourth section verifies the effectiveness of the proposed method through simulation results. The fifth section summarizes the main work of this paper.

2 Mathematical Model of PMSM

The stator voltage equation of surface-mounted PMSM (SPMSM) in the dq axis can be expressed as

$$\begin{cases} u_d = R \cdot i_d + L \frac{di_d}{dt} - \omega \cdot L \cdot i_q \\ u_q = R \cdot i_q + L \frac{di_q}{dt} + \omega \cdot L \cdot i_d + \omega \cdot \psi \end{cases} \quad (1)$$

where u_d , u_q , i_d , i_q stand for dq-axis stator voltage and current respectively. L, R, ψ stand for the inductance, resistance and flux-linkage of the SPMSM, respectively. ω stands for the electric angular velocity.

From (1), it can be seen that the voltage equations are coupled in the dq coordinate system, while the voltage equations are uncoupled in the $\alpha\beta$ coordinate system. Therefore the accurate discrete motor model is established in the $\alpha\beta$ coordinate system, as shown in Eq. (2). Meanwhile, the prediction model established on the $\alpha\beta$ axis can ignore the error of the voltage vector caused by the angular rotation in the coordinate transformation.

$$\begin{cases} u_\alpha = R \cdot i_\alpha + L \frac{di_\alpha}{dt} - \omega \cdot \psi \cdot \sin \theta \\ u_\beta = R \cdot i_\beta + L \frac{di_\beta}{dt} + \omega \cdot \psi \cdot \cos \theta \end{cases} \quad (2)$$

where u_α , u_β , i_α and i_β stand for $\alpha\beta$ -axis stator voltage and current respectively. θ stands for the electric angular.

Then the SPMSM mathematical model (2) can be Eulerian discretized to obtain the predicted current at time $(k+1)$. However, when the control frequency is low, the truncation error of the Eulerian discretization is large, and in order to improve the accuracy of the predicted current, the current at time $(k+1)$ can be

expressed :

$$i(k+1) = i(k) + \Delta i(T) \quad (3)$$

The current at time k can be obtained by current sampling. The amount of change in the current in the $\alpha\beta$ coordinate system at high speed over a control period is mainly influenced by the voltage and the reverse electromotive force. The voltage u in the stationary coordinate system can be considered to be constant over a control period. At the same time, at low control frequency, the angle of rotation of the counter electromotive force in one control cycle is not negligible. Then the change of current in a control cycle can be expressed as:

$$\begin{cases} \Delta i_a(T) = \int_0^T \frac{di_a}{dt} dt \approx \frac{-R \cdot T \cdot i_a(k) + T \cdot u_a(k) - \psi \cdot A}{T} \\ \Delta i_\beta(T) = \int_0^T \frac{di_\beta}{dt} dt \approx \frac{-R \cdot T \cdot i_\beta(k) + T \cdot u_\beta(k) - \psi \cdot B}{T} \end{cases} \quad (4)$$

where $A = \cos(\theta(k) + w \cdot T) - \cos(\theta(k))$, $B = \sin(\theta(k) + w \cdot T) - \sin(\theta(k))$.

From the above, current prediction model at time $(k+1)$ for the $\alpha\beta$ coordinate system can be obtained:

$$\begin{cases} i_a^p(k+1) = (1 - \frac{R \cdot T}{L}) \cdot i_a(k) + \frac{T}{L} \cdot u_a(k) - \frac{\psi}{L} \cdot A \\ i_\beta^p(k+1) = (1 - \frac{R \cdot T}{L}) \cdot i_\beta(k) + \frac{T}{L} \cdot u_\beta(k) - \frac{\psi}{L} \cdot B \end{cases} \quad (5)$$

At this point, the reference voltage can be obtained as follows.

$$\begin{cases} u_\alpha^* = \frac{L}{T} \cdot i_\alpha^*(k) - \frac{L-R}{T} \cdot i_a(k) + \frac{\psi}{T} \cdot A \\ u_\beta^* = \frac{L}{T} \cdot i_\beta^*(k) - \frac{L-R}{T} \cdot i_\beta(k) + \frac{\psi}{T} \cdot B \end{cases} \quad (6)$$

After minimizing the value function (7) the optimal voltage vector to be applied to the motor can be selected.

$$cf = |u_\alpha^* - u_\alpha^i| + |u_\beta^* - u_\beta^i| \quad (7)$$

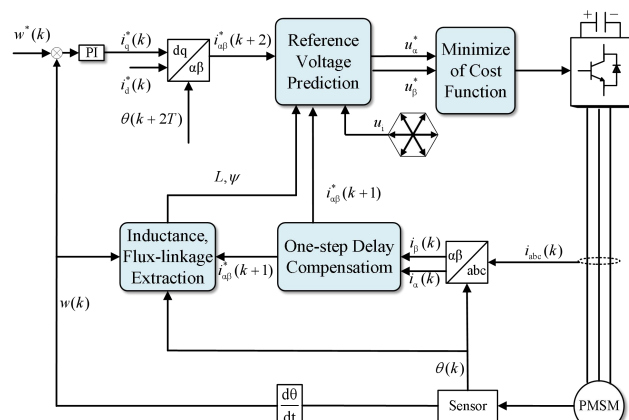


Fig. 1. The control diagram of the proposed method

3 The Proposed Method

The control block diagram of the proposed method in this paper is shown in Fig. 1, which consists of the following main parts: inductance and flux-linkage extraction, accurate reference voltage prediction, improved cost function optimization and one-step delay compensation. It is described in more detail below.

3.1 Inductance and Flux-linkage Extraction

From (5), the actual sampling and predicted currents at moment ($k+1$) can be obtained in Eq. (8) and (9) below, respectively:

$$\begin{cases} i_a(k+1) = \left(1 - \frac{R \cdot T}{L_0}\right) \cdot i_a(k) + \frac{T}{L_0} \cdot u_a(k) - \frac{\psi_0}{L_0} \cdot A \\ i_\beta(k+1) = \left(1 - \frac{R \cdot T}{L_0}\right) \cdot i_\beta(k) + \frac{T}{L_0} \cdot u_\beta(k) - \frac{\psi_0}{L_0} \cdot B \end{cases} \quad (8)$$

$$\begin{cases} i_a^p(k+1) = \left(1 - \frac{R \cdot T}{L}\right) \cdot i_a(k) + \frac{T}{L} \cdot u_a(k) - \frac{\psi}{L} \cdot A \\ i_\beta^p(k+1) = \left(1 - \frac{R \cdot T}{L}\right) \cdot i_\beta(k) + \frac{T}{L} \cdot u_\beta(k) - \frac{\psi}{L} \cdot B \end{cases} \quad (9)$$

where L , ψ stand for the model parameters of the SPMSM; L_0 , ψ_0 stand for the actual parameters of the SPMSM. The variation of the resistance parameter have almost no effect on the control performance of the MPC [10], so its effect on the proposed method can be neglected.

Similarly, the predicted and sampling values of the current at moment k can be obtained, and subtracting one from the other yields their current difference.

$$\begin{cases} E_\alpha = i_a^p(k) - i_a(k) \\ = RT\left(\frac{1}{L_0} - \frac{1}{L}\right) \cdot i_a(k-1) - T\left(\frac{1}{L_0} - \frac{1}{L}\right) \cdot u_a(k-1) \\ - \left(\frac{\psi}{L_0} - \frac{\psi_0}{L}\right) \cdot A \\ E_\beta = i_\beta^p(k) - i_\beta(k) \\ = RT\left(\frac{1}{L_0} - \frac{1}{L}\right) \cdot i_\beta(k-1) - T\left(\frac{1}{L_0} - \frac{1}{L}\right) \cdot u_\beta(k-1) \\ - \left(\frac{\psi}{L_0} - \frac{\psi_0}{L}\right) \cdot B \end{cases} \quad (10)$$

At this point, based on the known current, voltage data, accurate inductance and flux-linkage values can be extracted that are only relevant to the real-time detected values.

$$\begin{cases} \psi_0 = \frac{X \cdot D - Y \cdot C}{Y \cdot A - X \cdot B} \\ L_0 = \frac{(C + \psi_0 \cdot A) \cdot L}{X} \end{cases} \quad (11)$$

$$\begin{aligned} \text{where } X &= E_\alpha \cdot L + R \cdot T \cdot i_a(k-1) - u_a(k-1) \cdot T + \psi \cdot A \\ Y &= E_\beta \cdot L + R \cdot T \cdot i_\beta(k-1) - u_\beta(k-1) \cdot T + \psi \cdot B \\ C &= R \cdot T \cdot i_a(k-1) - T \cdot u_a(k-1), \quad D = R \cdot T \cdot i_\beta(k-1) - T \cdot u_\beta(k-1). \end{aligned}$$

3.2 Construction of the Cost Function

Substituting the extracted inductance and flux-linkage values into (6) gives the exact reference voltage.

$$\begin{cases} u_a = \frac{L_0}{T} \cdot i_a^*(k) - \frac{L_0 - R}{T} \cdot i_a(k) + \frac{\psi_0}{T} \cdot A \\ u_\beta = \frac{L_0}{T} \cdot i_\beta^*(k) - \frac{L_0 - R}{T} \cdot i_\beta(k) + \frac{\psi_0}{T} \cdot B \end{cases} \quad (12)$$

By substituting the obtained reference voltage into the cost function (7), the optimal voltage vector can be selected from the eight basic voltage vectors to be applied to the motor.

Traditional MPC cost function typically considers only single performance metrics such as current error, voltage error, or torque error, neglecting the impact of switching frequency. This method is effective at high switching frequencies but leads to a decline in control performance at low switching frequencies. To maintain good control performance at low switching frequencies, this paper proposes an improved cost function (13). This function includes the traditional current error term and adds a switching frequency penalty term (14).

$$cf = [u_a^* - u_a^i(k+1)]^2 + [u_\beta^* - u_\beta^i(k+1)]^2 + H \cdot J_1 \quad (13)$$

$$J_1 = |S_{abc}^2(k-1) - S_{abc}^1(k)| \quad (14)$$

where $S_{abc}^2(k-1)$ and $S_{abc}^1(k)$ represent the switching state of the bridge arm of the two-level three-phase inverter at ($k-1$) moment and k moment, respectively. H represents the weighting factor for the percentage of switching times

In adjacent sampling periods, only voltage vectors that significantly reduce the cost function value are selected, achieving optimized control at low switching frequencies. By incorporating this method, unnecessary switching actions can be effectively reduced, thereby decreasing switching losses and heat generation, while maintaining system robustness and high performance.

3.3 One-step Delay Compensation

A lower switching frequency may result in a higher sampling delay. At higher sampling delays, the error of the system sampling data increases, which leads to a degradation of the system control performance. Therefore, delay compensation is necessary.

$$\begin{cases} u_a = \frac{L}{T} \cdot i_a^*(k+1) - \frac{L-R}{T} \cdot i_a(k+1) + \frac{\psi_r}{T} \cdot A \\ u_b = \frac{L}{T} \cdot i_b^*(k+1) - \frac{L-R}{T} \cdot i_b(k+1) + \frac{\psi_r}{T} \cdot B \end{cases} \quad (15)$$

$$\begin{cases} \hat{i}_a(k+1) = \hat{i}_a \cdot e^{j\theta_0} \\ \hat{i}_b(k+1) = \hat{i}_b \cdot e^{j\theta_0} \end{cases} \quad (16)$$

where $\theta_0 = \theta(k) + 2wT$.

In summary, by reconstructing the cost function and integrating the improved predictive model and control strategy, this paper proposes a method that significantly enhances the control performance of PMSMs at low switching frequencies. This method not only reduces switching losses and heat generation but also maintains the system's efficiency and reliability, improving system robustness and control performance.

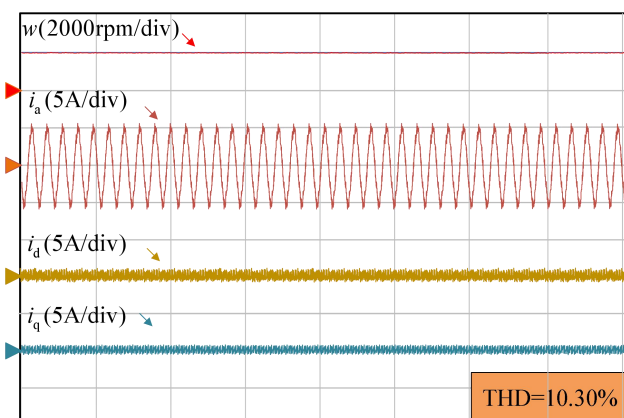
4 Simulation Experiment

To confirm the proposed method's effectiveness, simulation results are conducted utilizing the MATLAB/Simulink tool. Table I presents the relevant parameters employed in the simulation. The simulation result graph depicts curves representing rotor speed (ω_r), dq axis current (i_d , i_q), and stator single-phase current (i_a).

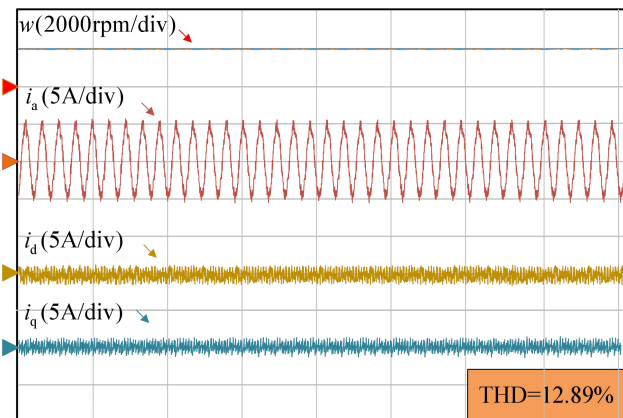
TABLE I
PARAMETERS OF SPMSM

Symbol	Value	Symbol	Value
U_{dc} (V)	310	T (s)	0.0001
R (Ω)	3	T_N (N·m)	6
L (mH)	8.5	n_N (r/min)	2000
ψ_r (Wb)	0.24	p	3

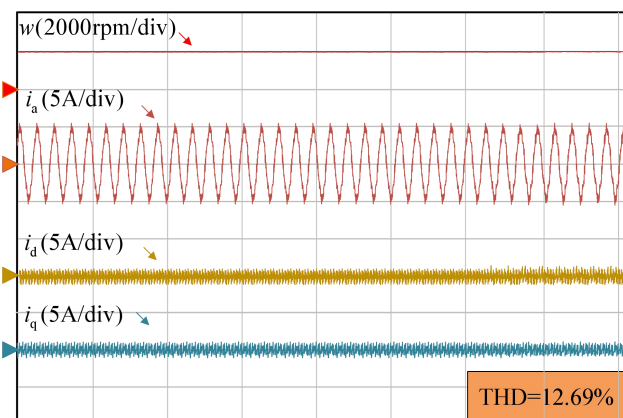
Fig. 2 demonstrates the experimental results of the steady-state performance of the proposed method and the traditional method under high-speed operating conditions. According to Fig. 2(a) and (d), when the



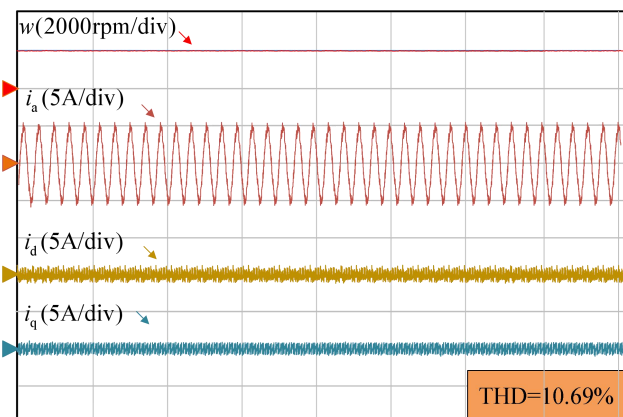
(a)



(b)



(c)



(d)

Fig. 2. Steady-state simulation results at 2000rpm, rated torque (a) The proposed method with accurate parameters ($H=0$) (b) The proposed method with accurate parameters ($H\neq 0$) (c) The proposed method with mismatched parameters ($H\neq 0$) (d) The traditional method with accurate parameters.

weighting factor H of the proposed method is 0, its total harmonic distortion (THD) is 10.30%, which is better than that of the traditional method, indicating that the proposed method has the validity of an accurate model. When the parameters are mismatched, it can be seen from Fig. 2(b) and (c) that

the THD of the proposed method remains stable and the current ripple does not increase, demonstrating good parameters robustness. In addition, when the weighting factor H plays a role, the average switching frequency of the proposed method in Fig. 2(b) is about 730 Hz, indicating that the proposed method can operate stably at low switching frequencies. Moreover, as illustrated in Fig. 3, under rated load conditions, the proposed method effectively limits the rise in average switching frequency across various speed conditions.

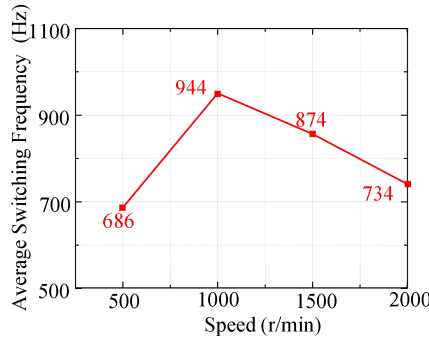


Fig. 3. The performance of average switching frequency at different speeds and rated load.

Fig. 4 demonstrates the inductance and flux-linkage parameters updated in real time under parameter mismatch, further proving the effectiveness of the proposed method.

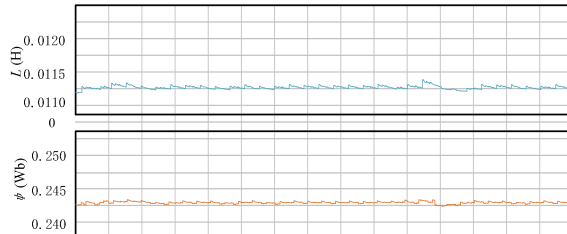
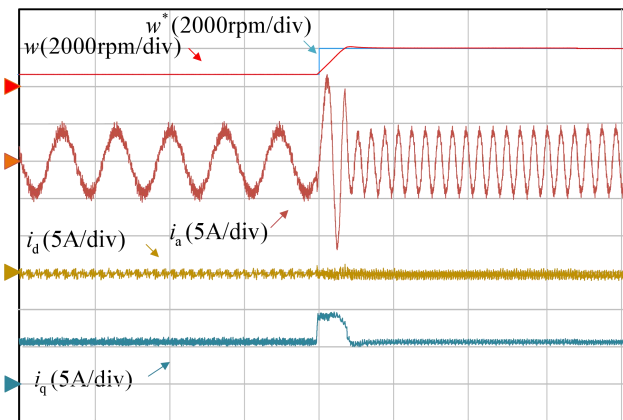
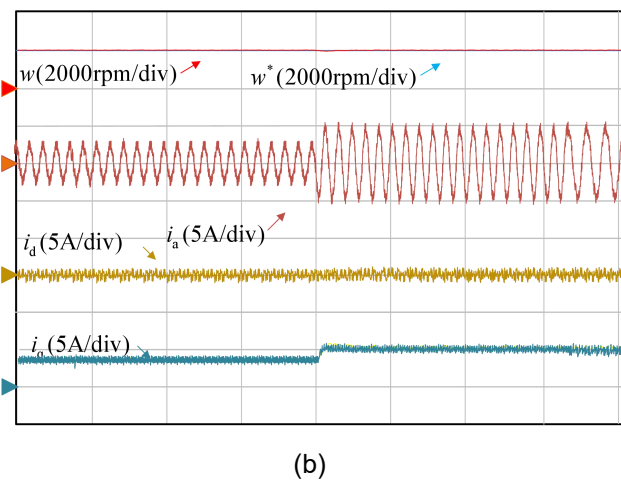


Fig. 4. Parameter extraction results of inductance and flux-linkage

Fig. 5 shows that the PMSM reaches steady state in a very short time for both sudden speed and torque changes. This demonstrates the superior performance of the proposed method in terms of dynamic response.



(a)



(b)

Fig. 5. Dynamic simulation results (a) Speed increase from 500rpm to 2000rpm at rated torque (b) Torque increase from 3Nm to 6Nm at rated speed.

In summary, the above simulation results indicate that the proposed method demonstrates excellent dynamic and steady-state performance at low switching frequencies, enhances system robustness, and achieves satisfactory control effects.

5 Conclusions

The main contributions of this paper include: 1) improving the robustness of the PMSM at low switching frequencies; 2) establishing an accurate mathematical model and a real-time detection model for the parameters, and improving the value function to enhance the control performance of the system; and 3) verifying the feasibility and superiority of the method through simulation.

6 References

- [1] X. Zhang, B. Hou and Y. Mei, "Deadbeat Predictive Current Control of Permanent-Magnet Synchronous Motors with Stator Current and Disturbance Observer," in IEEE Transactions on Power Electronics, vol. 32, no. 5, pp. 3818-3834, May 2017, doi: 10.1109/TPEL.2016.2592534.
- [2] X. Zhang and L. Xu, "A Simple Motor-Parameter-Free Model Predictive Voltage Control for PMSM Drives Based on Incremental Model," in IEEE Journal of Emerging and Selected Topics in Power Electronics, doi: 10.1109/JESTPE.2024.3387454.
- [3] C. Gong, Y. Hu, M. Ma, L. Yan, J. Liu and H. Wen, "Accurate FCS Model Predictive Current Control Technique for Surface-Mounted PMSMs at Low Control Frequency," in IEEE Transactions on Power Electronics, vol. 35, no. 6, pp. 5567-5572, June 2020, doi: 10.1109/TPEL.2019.2953787.
- [4] H. Le, A. Dekka and D. Ronanki, "Low Switching Frequency FCS-MPC Technique for Four-Level Inverters," 2023 IEEE Energy Conversion Congress and Exposition (ECCE), Nashville, TN,

- USA, 2023, pp. 3062-3068, doi: 10.1109/ECCE53617.2023.10362772.
- [5] X. Zhang and J. Li, "Model Predictive Switching Control for PMSM Drives," in IEEE Journal of Emerging and Selected Topics in Power Electronics, 2022, doi: 10.1109/JESTPE.2022.3212775.
- [6] X. Zhang, H. Bai and M. Cheng, "Improved Model Predictive Current Control With Series Structure for PMSM Drives," in IEEE Transactions on Industrial Electronics, vol. 69, no. 12, pp. 12437-12446, Dec. 2022.
- [7] Y. Wang, Z. Xue, G. Luo and Z. Chen, "A Time-Delay Compensation Method for PMSM Sensorless Control System under Low Switching Frequency," IECON 2019 - 45th Annual Conference of the IEEE Industrial Electronics Society, Lisbon, Portugal, 2019, pp. 880-885, doi: 10.1109/IECON.2019.8927321.
- [8] Y. Zhang and H. Yang, "Model Predictive Torque Control of Induction Motor Drives With Optimal Duty Cycle Control," in IEEE Transactions on Power Electronics, vol. 29, no. 12, pp. 6593-6603, Dec. 2014, doi: 10.1109/TPEL.2014.2302838.
- [9] Y. Zhang and Y. Bai, "Model predictive control of three-level inverter-fed induction motor drives with switching frequency reduction," IECON 2017 - 43rd Annual Conference of the IEEE Industrial Electronics Society, Beijing, China, 2017, pp. 6336-6341, doi: 10.1109/IECON.2017.8217103.
- [10] X. Zhang, Z. Liu, P. Zhang and Y. Zhang, "Model Predictive Current Control for PMSM Drives Based on Nonparametric Prediction Model," in IEEE Transactions on Transportation Electrification, vol. 10, no. 1, pp. 711-719, March 2024, doi: 10.1109/TTE.2023.3293512.